STRONG MOTION SIMULATION AND MODELING OF THE 2001 GEIYO (M_J6.7), JAPAN, EARTHQUAKE, USING THE EMPIRICAL GREEN'S FUNCTION METHOD

M. Ohori[1]

[1] *Researcher, Dept. of Oceanfloor Network System Development for Earthquakes and Tsunamis, Japan Agency for Marine-Earth Science and Technology, Yokohama, Japan*
Email: ohorim@jamstec.go.jp

ABSTRACT :

In this study, I carried out source parameter estimation and strong motion simulation of the 2001 Geiyo earthquake (M_J6.7), Japan. Data obtained at 10 KiK-net stations located at 19 to 66 km in epicentral distance is used. To focus on the source modeling without consideration about nonlinearity of soft surface layers, borehole records are targeted. First, to derive rough estimates of basic source parameters, I inverted spectral amplitude from the S-wave main portion of the mainshock and 12 aftershocks (M_J3.5 to 5.0). The moment magnitude, the corner frequency and the stress drop for the mainshock were estimated to be 6.3, 0.5 Hz and 377 bar, respectively. Next, using data from the largest aftershock as the empirical Green's function, I estimated the relative moment release distribution on the fault plane and simulated the strong motion records targeting the mainshock in a range of 0.3 to 10 Hz. Waveform matching between synthesis and observed data is satisfactory. The maximum amplitudes of observed horizontal components from 10 stations were in a range of 24 to 123 gal in acceleration and 1.6 to 8.5 kine in velocity. At most of the stations, the observed maximum amplitudes were simulated successfully within a factor of 2.

KEYWORDS: The 2001 Geiyo Earthquake, Empirical Green's Function, Source Modeling

1. INTRODUCTION

The 2001 Geiyo earthquake (M_J6.7) ruptured in the Philippine Sea slab beneath the Seto Inland Sea of Japan at a depth (51 km) on March 24, 2001. The source mechanism of the event was normal faulting. This earthquake released high frequency energy to the southwest Japan and caused 2 deaths and injured 288 people. 70 houses were collapsed and 774 houses were damaged (Cabinet Office, 2001). The study on the source modeling and strong motion simulation for the earthquake is considered to be significant from both seismological and engineering points of views.

In this study, I carried out source parameter estimation and strong motion simulation with use of the empirical Green's function method. Fortunately, the KiK-net, one of the strong motion networks operated by the National Research Institute of Earth Science and Disaster Prevention (NIED), has been just started since August, 2000, seven months before the event. I targeted 10 KiK-net stations located at 19 to 66 km in epicentral distance. The KiK-net record the three-component data simultaneously at the bottom of borehole and the surface at the same site. To focus on the source modeling without any consideration about nonlinear behavior of soft surface layers at many sites reported in previous studies [e.g. Kanno and Miura (2005)], borehole records were used.

First, I inverted spectral amplitude of the S-wave main portion from mainshock and 12 aftershocks (M_J 3.5 to 5.1) and derived rough estimates of basic source parameters characterizing the omega-square source spectrum by Brune (1970). Second, I carried out strong motion simulation based on the empirical Green's function method. A simple fault plane of 30 km by 18 km with strike of 180 deg. and dip of 60 deg. was assumed with reference of source models in previous studies [e.g. Kikuchi and Yamanaka (2001), Sekiguchi and Iwata (2001), Nozu (2001) and Kakehi (2004)]. Using data from the largest aftershock as the empirical Green's function, I estimated the relative moment release distribution on the fault plane and simulated the strong motion records from the mainshock.

2. EVENTS AND STATIONS

In Figure 1, locations of the mainshock (M_J6.7, labeled as Event 1) and 12 aftershocks (M_J3.5 to 5.0, Events 2-13) of the Geiyo earthquake are shown. The focal mechanism solutions of events determined by the F-net are inserted. Also, 10 KiK-net stations, which was used in Koketsu and Furumura (2002), are plotted with up-side-down solid triangles. These stations are surrounding the rupture area of the mainshock and their recordings are carried out not only at the surface but also at the borehole, as mentioned above. They are located at 19 km to 66 km in epicentral distance for the mainshock, and the S-wave velocity at their boreholes (Vs_{max}) are ranging from 2000 m/s to 2900 m/s, except for two stations, HRSH07, EHMH04 with the Vs_{max} of 1200 m/s and 700 m/s, respectively. As for the mainshock, the nonlinear behavior of soft surface layers are pointed out [e.g. Kanno and Miura (2005)]. On the other hand, the data recorded at close distance from the source is considered to be rich in source characteristics. Therefore, to focus on the source modeling without any consideration about nonlinearity of surface layers, I used borehole data instead of surface data.

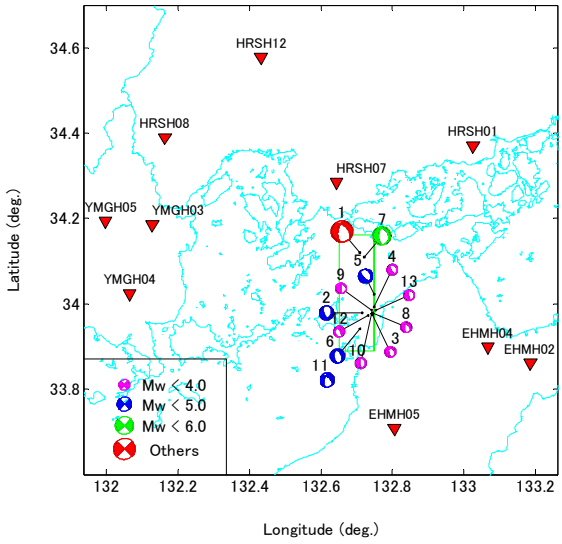

Figure 1 Map showing location of epicenters and stations targeted in this study

3. INVERSION OF SPECTRAL AMPLITUDE

3.1 Data Processing

To have rough estimates for the source parameters, the spectral amplitude inversion was carried out. I took 20 second time window for the S-wave portions from the NS and EW components. The beginning and the end of the window were tapered with 1 second cosine taper. Then, I calculate the Fourier transform from a complex signal x(t)+iy(t), where x(t) and y(t) denote two orthogonal horizontal components. The amplitude spectrum was smoothed by a Parzen window with a width having frequency dependence: given by 0.1f with the minimum of 0.1 Hz and the maximum of 1.0 Hz. The spectral amplitude between 0.1 and 20 Hz was targeted in the spectrum inversion.

3.2 Analytical Method

Analytical procedure of the spectrum inversion employed in this study was almost the same as the method by Iwata and Irikura (1986), except that Q_s-value (quality factor of the S-wave) along the propagation path was given a priori after preliminary analyses.

Let us consider the spectral expression of the ground motion. The spectral amplitudes at the j-th station from the i-th event, $O_{ij}(f)$ can be given by

$$O_{ij}(f) = S_i(f)G_j(f)\frac{1}{R_{ij}}\exp\left(\frac{-\pi f R_{ij}}{Q_s(f)V_s}\right) \quad (1)$$

where $S_i(f)$, $G_j(f)$ and $Q_s(f)$ represent the source spectrum, the site amplification, and quality factor along the path from source to station. Also, R_{ij} and V_s represent the corresponding hypocentral distance and the average S-wave velocity from source and station. V_s was assumed to be 3.8 km/s. The equation (1) can be rewritten as

$$\overline{O}_{ij}(f) = S_i(f)G_j(f) \quad (2)$$

where $\overline{O}_{ij}(f)$ is the path-effect corrected spectral amplitude given by

$$\overline{O}_{ij}(f) = R_{ij}O_{ij}(f)\exp\left(\frac{\pi f R_{ij}}{Q_s(f)V_s}\right) \quad (3)$$

We take the logarithm of the equation (2) and derive the following expression:

$$\log_{10}\overline{O}_{ij}(f) = \log_{10}S_i(f) + \log_{10}G_j(f) \quad (4)$$

The unknowns to be solved in the above equation are $S_i(f)$, $G_j(f)$ and $Q_s(f)$. As previously mentioned, in this study, $Q_s(f)$ was treated to be given. I tested several $Q_s(f)$ models in preliminary analyses and examined the spectrum matching between the synthesized spectrum and observed ones. As a result, $Q_s(f) = 81f^{0.85}$ was seemed to be appropriate in this study. Therefore unknowns were reduced to two parameters, $S_i(f)$ and $G_j(f)$. Considering M events and N stations in total, M by N simultaneous equations are constructed for each frequency. These equations can be solved with the nonnegative least square method by Lawson and Hansen (1974). To solve the equations with a constraint of $G_j(f) \geq 2$, $G_j(f)$ was substituted by $2G'_j(f)\left(=G_j(f)\right)$ because in solving the logarithmic solution, the nonnegative constraint of $\log_{10}G'_j(f) \geq 0$ corresponds to $G'_j(f) \geq 1$. Moreover, the equation (1) was normalized by the minimum amplitude of $\overline{O}_{ij}(f)$ for each frequency.

3.3 Results

In Figures 2a and 2b, the inverted source spectra for 13 events are shown with bold jagged lines. The source acceleration and displacement spectrum are scaled into those at 1 km in hypocentral distance. In Figure 2c, the spectral ratios between the mainshock and each aftershock are shown.

In order to determine basic source parameters [the moment magnitude M_W (or the seismic moment), the corner frequency, the stress drop], I fit the theoretical source acceleration spectrum with inverted one. The source acceleration spectrum used here is the omega-square model by Brune (1970) combined with a high frequency cut-off filter, given by

$$S(f) = \frac{r_s M_0}{4\pi\rho\beta^3 R}\frac{(2\pi f)^2}{1+\left(\frac{f}{f_c}\right)^2}\frac{1}{1+\left(\frac{f}{f_{\max}}\right)^n} \quad (5)$$

where r_s is the average radiation pattern for the S-wave, R is the hypocentral distance. ρ and β denote the density and the S-wave velocity in the source layer. $f_{\max}$ and n denote parameters for a high frequency cut-off filter. M_0 and f_c represent the seismic moment and the corner frequency. The stress drop is given by

$$\Delta\sigma_s = \left(\frac{f_c}{4.9 \times 10^6 \beta} \right)^3 M_0 \qquad (6)$$

where R_s, R, ρ and β were assumed to be 0.63, 1 km, 3.1g/cm^3 and 4.62 km/s, respectively. M_0 and f_c were determined by fitting the inverted source spectrum with the model. n was assumed to be 1 and $f_{\max}$ was determined in a range of 14 to 24 Hz by eye inspection.

In Figure 2, the model source spectra were plotted with thin smooth lines. The corner frequency for each event was plotted with an open circle. The model spectra agree well with the inverted ones so that the scaling law based on the omega-square model was considered to be valid among targeted events in this study.

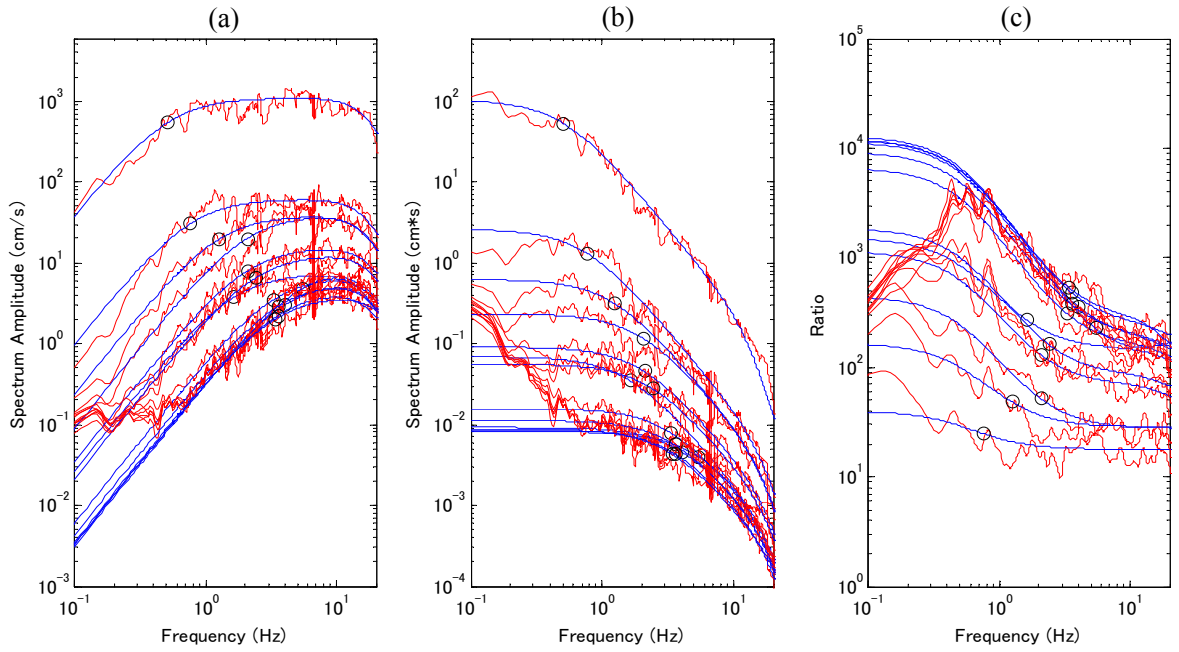

Figure 2 Comparison between inverted and theoretical source spectra

Table 1 Summary of the estimated results of source parameters

Event	JMA				F-net	Spectrum Inversion		
	Date (y:m:d)	Clock (h:m:s)	Depth (km)	M_J	M_W	M_W	f_c (Hz)	$\Delta\sigma$ (bar)
1	2001:03:24	15:27:54.1	51.4	6.7	6.8	6.3	0.5	377
2	2001:03:24	22:37:33.6	46.9	4.1	4.1	4.2	1.6	8
3	2001:03:25	02:19:52.3	49.5	3.8	3.6	3.8	3.3	16
4	2001:03:25	09:10:54.1	50.1	3.8	3.5	3.6	5.4	35
5	2001:03:25	19:19:11.4	51.3	4.4	4.4	4.5	2.1	54
6	2001:03:26	02:16:00.3	47.6	3.9	4.1	4.3	2.1	22
7	2001:03:26	05:40:53.2	49.3	5.0	5.1	5.2	0.8	32
8	2001:03:26	18:59:23.3	49.4	3.9	3.5	3.6	4.1	16
9	2001:06:30	17:13:19.9	47.3	4.0	3.6	3.7	3.6	14
10	2001:08:24	21:44:32.5	47.8	4.3	4.0	4.1	2.4	21
11	2002:03:25	22:58:17.2	46.2	4.7	4.7	4.8	1.2	32
12	2002:12:20	03:48:58.2	46.0	3.8	3.6	3.6	3.6	11
13	2004:03:10	04:56:37.4	42.5	3.6	3.6	3.6	3.4	9

In Table 1, the estimated results of source parameters are summarized. The moment magnitude (M_W), the corner frequency, and the stress drop were estimated to be 6.3, 0.5 Hz, and 377 bar for the maishock, and 5.2, 0.8 Hz, and 32 bar for the largest aftershock (Event 7 in Figure 1).

4. SIMULATION OF THE MAINSHOCK

4.1 Fault Plane Discretization

Referring to the focal mechanism solutions, aftershock distribution, and waveform inversion results in previous studies [e.g. Kikuchi and Yamanaka (2001), Sekiguchi and Iwata (2001), Nozu (2001), and Kakehi (2005)] , I assumed simple rectangular fault plane with 30 km in length and 18 km in width, on which the mainshock hypocenter was located as a rupture point. See Figure 1. The strike and dip of the fault plane was set to 180 deg. and 60 deg., respectively. The depth of the fault plane is 45 km at top and 60 km at bottom.

To express rupture propagation from the hypocenter to the whole fault plane, it was divided into 10 by 6 subfaults with the size of 3 km by 3 km. Rupture velocity of 3.0 km/s was selected after comparison of the results with rupture velocity between 2.5 km/s and 3.5 km/s.

4.2 Method and Analytical Condition

Since a pioneering work by Hartzell (1978), the empirical Green's function method has been recognized as a useful technique to synthesize strong ground motion and extended in various ways by various researchers. Among them, I selected the method proposed by Dan and Sato (1998), because theirs can easily incorporate the variable-slip rupture model with the empirical Green's function method to simulate the broadband strong ground motion.

In this study, I used the data from the largest aftershock as the empirical Green's function. Note that the mainshock and aftershock have difference in the moment magnitude (or the seismic moment), the corner frequency, and the stress drop, as summarized in Table 1. Also, the rupture area of the aftershock was evaluated to be 2.2 km in radius whereas the equivalent radius of each subfault modeled here was about 1.7 km. The Dan and Sato's method can compensate such differences in frequency domain and provide the element wave from each subfault. Considering difference in timing and geometrical spreading between each subfault and the station, every element wave from each subfault can be summed as the strong ground motion from the whole fault plane.

From a quick look at Figure 2c, the source spectrum ratio between the mainshock and the largest aftershock seemed to obey the scaling law based on the omega-square model [Brune (1970)] at a frequency higher than 0.3 Hz. Also, as mentioned in previous chapter, $f_{\max}$ is at least higher than 10 Hz, although it varies from event to event. In the following simulation, the data from the both mainshock and aftershock events was band-pass filtered between 0.3 and 1 Hz in waveform inversion and between 0.3 and 10 Hz in forward modeling.

4.3 Results

Firsty, prior to the waveform simulation. I carried out waveform inversion to derive the rupture model using the element wave from each subfault as the empirical Green's function. The acceleration data was twice integrated into displacement with a bandpass-filter ranging from 0.3 to 1Hz. Simple inversion allowing each subfault to rupture once was carried out using the nonnegative least square method by Lawson and Hansen (1974). In Figure 3, the relative moment release on the fault plane is shown. Contour lines are plotted with an unit step corresponding to the seismic moment of the largest aftershock (Event 7). A solid star inserted represents a rupture starting point (the mainshock hypocenter) On the basis that the Event 7 is an earthquake of M_W5.2, the mainshock can be evaluated to be M_W6.5. Note that the relative moment release distribution in Figure 3 is similar with the result from more detailed analysis [Figure 7 in Kakehi (2004)].

Next, using the relative moment release model in Figure 3, the strong ground motion for the mainshock was synthesized in a frequency range from 0.3 to 10 Hz. In Figure 4, the maximum amplitudes for the mainshock are compared between the synthesis and data in acceleration (a), velocity (b), and displacement (c). Also, waveforms for selected stations are shown in Figure 5 as examples. As example results, acceleration, velocity,

and displacement waveforms are plotted for YMGH03 (a) and EHMH04 (b). In each diagram, nine traces are drawn: top three traces are the observed data for the Event 7 (EGF), middle three are the synthesized ones (Syn.), and others are the observed data for the mainshock (Obs.). Every three traces are aligned in the order of NS-, EW-, and UD-components. Numerals at the end of traces are absolute maximum amplitudes.

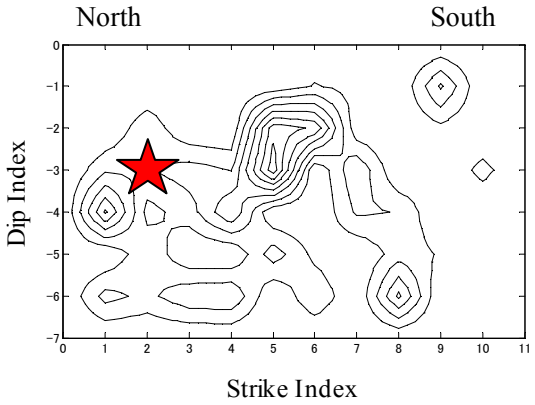

Figure 3 Relative moment release distribution on the fault plane for the mainshock

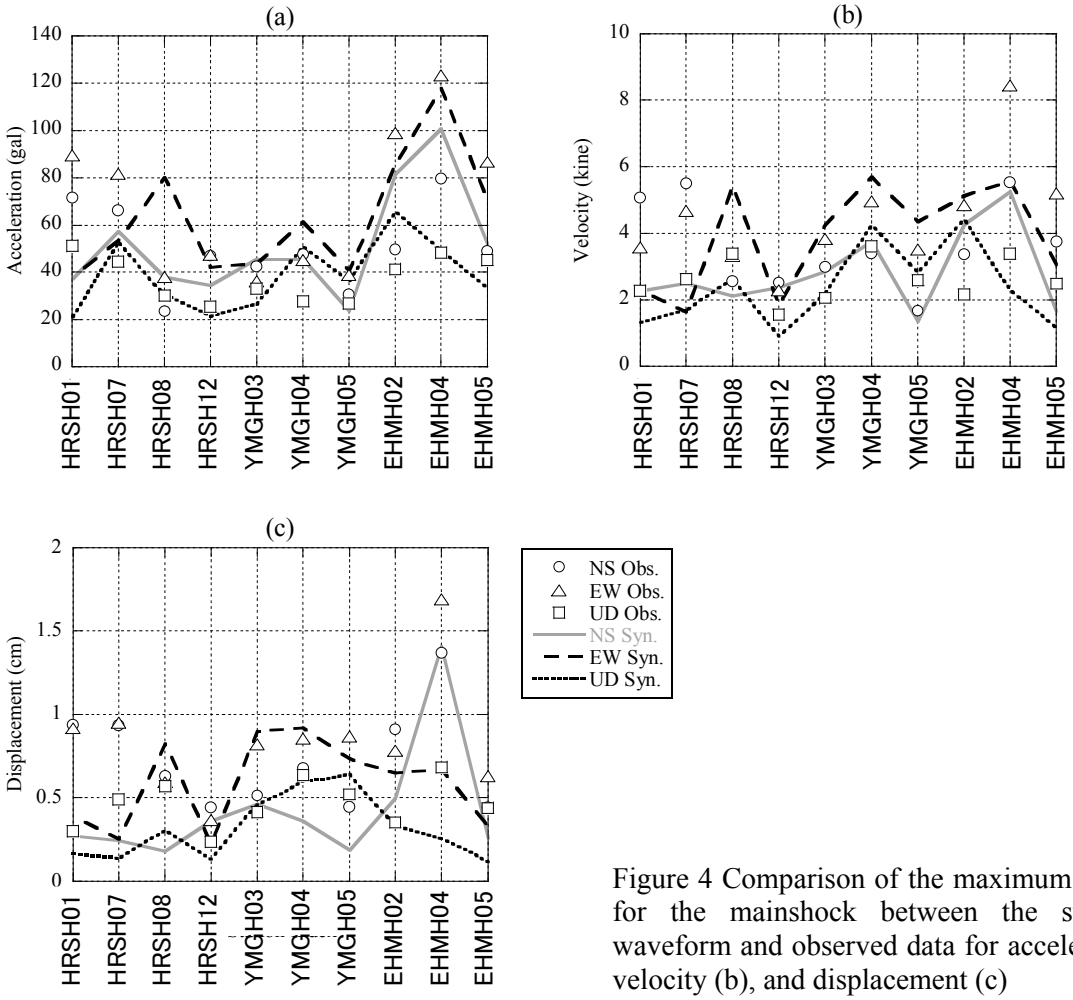

Figure 4 Comparison of the maximum amplitude for the mainshock between the synthesized waveform and observed data for acceleration (a), velocity (b), and displacement (c)

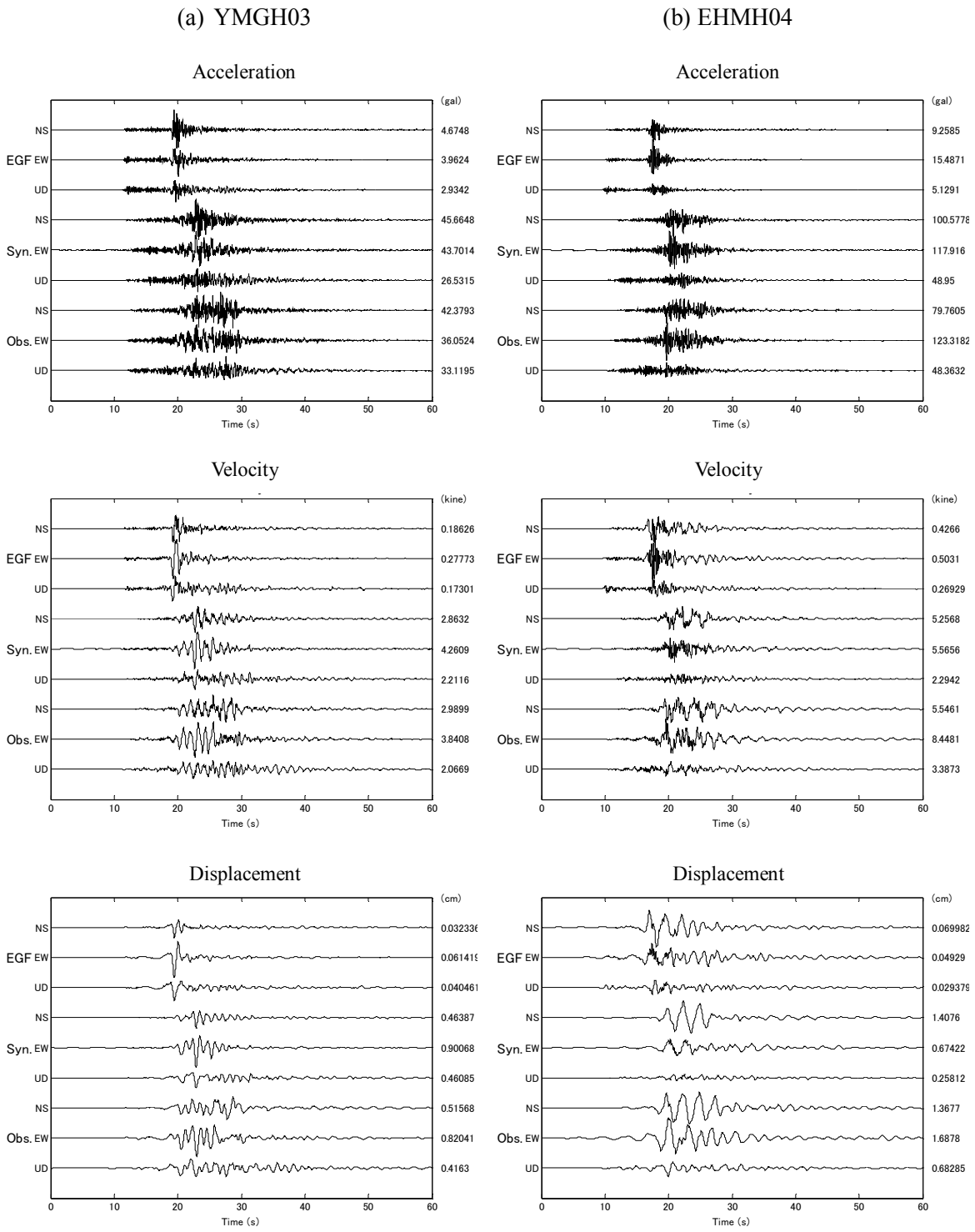

Figure 5 Comparison of synthesized waveforms and observed data

On the whole, waveform matching between synthesis and observed data is satisfactory. The maximum amplitudes of observed horizontal components from 10 stations were in a range of 24 to 123 gal in acceleration and 1.6 to 8.5 kine in velocity. Present simulation reproduced most of the observed maximum amplitudes within a factor of 2. At two stations, HRSH01 and HRSH07, the simulation underestimated the observed data in most of the components. It may be partially attributed to isolated later phases appearing in the observed waveforms at

these stations. Similar result was found in Sekiguchi and Iwata (2001). They suggested that the more complex rupture history was required for the simulation of the stations located in the northern direction from the rupture area.

5. CONCLUSIONS

The source parameters of the 2001 Geiyo earthquake (M_J6.7) was estimated by the spectrum inversion using the KiK-net borehole data. The moment magnitude, the corner frequency, and the stress drop were estimated to be 6.3, 0.5 Hz, and 377 bar for the maishock, and 5.2, 0.8 Hz, and 32 bar for the largest aftershock. Next, based on the obtained source parameters, the empirical Green's function method was applied to simulate the strong ground motion for the mainshock. Element waves evaluated from the largest aftershock data were used for the waveform inversion and the strong motion simulation. Comparison of synthesized waveforms and observed data shows a good agreement.

ACKNOWLEDGEMENTS

In this study, I used the strong motion data of the KiK-net and the source parameter information of the F-net, operated by the National Research Institute for Earth Science and Disaster Prevention. My sincere gratitude is given to whom it may concern.

REFERENCES

Brune, J. N. (1970), Tectonic Stress and the Spectra of Seismic Shear Waves from Earthquakes, *J. Geophys. Res*, **81**, 4997-5009.

Cabinet Office, Government of Japan (2001), http://www.buosai.go.jp/kinkyu/akinada/akinada0919.pdf.

Dan, K. and Sato,T. (1998), Strong-Motion Prediction by Semi-Empirical Method based on Variable-Slip Rupture Model of Earthquake Fault, *J. Struct. Constr. Eng.*, Architecture Insitute of Japan, **509**, 49-60.

F-net (Broadband Seismograph Network) operated by National Research Institute for Earth Science and Disaster Prevention, http://www.fnet.bosai.go.jp/freesia/index.html.

Hartzell, S. H., (1978), Earthquake aftershocks as Green's functions, *Geophys. Res. Lett.*, ***5***, 1-4.

Iwata, T. and Irikura, K. (1986), Sparation of Source, Propagation and Site Effects from Observed S-waves, *Zisin 2*, **39**, 579-593.

Kakehi, Y. (2004), Analysis of the 2001 Geiyo, Japan, Earthquake using High-density Strong Motion Data: Detailed Rupture Process of a Slab Earthquake in a Medium with a Large Velocity Contrast, *J. Geophys. Res.*, **109**, B08306, doi:10.1029/2004JB002980.

Kanno, T., and Miura, K. (2005), Evaluation of Site Effects during the 2001 Geiyo Earthquake in Hiroshima Prefectrure, *J. Struct. Constr. Eng.*, Architecture Insitute of Japan, **597**, 151-157.

KiK-net (Digital Strong-Motion Seismograph Network) operated by National Research Institute for Earth Science and Disaster Prevention, http://www.kik.bosai.go.jp/kik/.

Kikuchi, M. and Yamanaka, K. (2001), http://wwweic.eri.u-tokyo.ac.jp/EIC/EIC_News/010324.html.

Koketsu, K. and Furumura, T. (2002), The Distribution of Strong Motion from the 2001 Geiyo Earthquake and the Deep Underground Structure , *Zisin 2*, **55**, 97-105.

Lawson, C. L. and Hanson, D. J. (1974), Solving least squares problems, Prentice-Hall Inc., Englewood Cliffs, New Jersey, 337 pp.

Nozu,A. (2001), http://www.pari.go.jp/information/news/h13d/jisin/geiyo/geiyo2/geiyo2.htm.

Sekiguchi, H. and Iwata, T. (2001), http://sms.dpri.kyoto-u.ac.jp/iwata/zisin/geiyo-e/html.